

Dynamical replica analysis of disordered Ising spin systems on finitely connected random graphs

J.P.L. Hatchett,¹ I. Perez Castillo,² A.C.C. Coolen,³ and N.S. Skantzos⁴

¹Laboratory for Mathematical Neuroscience, RIKEN Brain Science Institute, Wako, Saitama 351-0198, Japan

²Rudolf Peirls Center for Theoretical Physics, University of Oxford, 1 Keble Road, Oxford OX1 3NP, UK^y

³Department of Mathematics, King's College, University of London, The Strand, London WC2R 2LS, UK^z

⁴Instituut voor Theoretische Fysica, Katholieke Universiteit Leuven, Celestijnenlaan 200, DB-3001 Leuven, Belgium^x

(Dated: April 14, 2024)

We study the dynamics of macroscopic observables such as the magnetization and the energy per degree of freedom in Ising spin models on random graphs of finite connectivity, with random bonds and/or heterogeneous degree distributions. To do so we generalize existing implementations of dynamical replica theory and cavity field techniques to systems with strongly disordered and locally tree-like interactions. We illustrate our results via application to the dynamics of e.g. Ising spin-glasses on random graphs and of the overlap in finite connectivity Sourlas codes. All results are tested against Monte Carlo simulations.

PACS numbers: 75.10.N4, 05.20.-y, 64.60.Cn

Recent years have witnessed a surge of interest in the study of finitely connected disordered spin systems. From a physical point of view, despite their lack of a realistic geometry and their mean-field nature, the finite number of neighbours per spin in such models does give rise to a non-trivial local geometry and ensuing artifacts. Here we simply regard the random bond finite connectivity Ising spin system as the archetypal interacting particle model on a disordered random graph. Such models are important in the understanding of algorithmic complexity in theoretical computer science [1, 2, 3], and also underlie recent theoretical advances for an important class of error correcting codes [4, 5, 6]. It has been shown that the tuning of the degree distribution and/or the connectivity strengths in complex networks can lead to atypical mean-field critical phenomena [7, 8, 9], and they are now increasingly and fruitfully used for modeling neural, social, internet, gene regulatory and proteomic networks [10, 11, 12, 13, 14]. While our quantitative understanding of the equilibrium properties of these systems is quite advanced (see e.g. [15, 16]), the tools available for studying their non-equilibrium behaviour are comparatively poor. There has been some progress in applying the path integral techniques of [17] to spherical and related models [18], and to Ising models with parallel spin updating [19, 20]. Generalizing such approaches to Ising spin models with Glauber-type dynamics requires the treatment of non-trivial functional order parameters which have, as yet, not been adequately controlled. An alternative approach, which we follow here, is to generalize the techniques of dynamical replica theory (DRT) [21, 22], together with the cavity field concept, to finitely connected disordered spin systems. This approach has already proven fruitful for weakly disordered dilute ferromagnets [23] where each spin is effectively in an identical environment. In this letter, in contrast, we study the dynamics of strongly disordered versions of finitely

connected Ising systems, where each spin is in a highly heterogeneous environment, due to the presence of either random bonds or nodes with variable degrees.

Our model consists of N Ising spins $s_i \in \{-1, 1\}$; $i = 1, \dots, N$, whose mutual interactions are characterized by a range-free symmetric adjacency matrix with entries $c_{ij} \in \mathbb{R}$ and symmetric bonds $J_{ij} \in \mathbb{R}$. We define $c_{ii} = 0$, and draw the bond strengths J_{ij} i.i.d. from some distribution $Q(J)$. The probability of finding any state $s = (s_1, \dots, s_N)$ of the system at time t is given by the measure $p_t(s)$, which evolves as the spins align asynchronously and stochastically to their local fields, according to a Glauber dynamics in the form of the master equation

$$\frac{d}{dt} p_t(s) = \sum_{k=1}^N [p_t(F_k s) w_k(F_k s) - p_t(s) w_k(s)] \quad (1)$$

where $F_k s = (s_1, \dots, s_k, \dots, s_N)$ is the k th spin-flip operator and the transition rates $w_k(s)$ have the standard form

$$w_k(s) = \frac{1}{2} [1 - s_k \tanh[h_k(s)]] g \quad (2)$$

with the local fields $h_i(s) = \sum_{j \neq i} c_{ij} J_{ij} s_j$. This process evolves toward equilibrium, with the Boltzmann measure and with Hamiltonian

$$H(s) = \sum_{i < j} c_{ij} J_{ij} s_i s_j - \sum_i s_i \quad (3)$$

Following the procedure outlined for fully connected systems [21, 22] we consider the evolution of two macroscopic observables, the magnetization $m_t(s) = N^{-1} \sum_i s_i$ and the internal energy $e(s) = N^{-1} \sum_{i < j} c_{ij} J_{ij} s_i s_j$. We will abbreviate $(m; e)$. One easily derives a Kramers-Moyal_P(KM) expansion for their probability density $P_t(\cdot) = \sum_s p_t(s) [\cdot](s)$. On finite times

one finds that only the Liouville term in the KM expansion survives the thermodynamic limit, so the observables $(m; e)$ evolve deterministically, i.e. $\lim_{N \rightarrow \infty} P_t(\cdot) = [\cdot]_t$ with

$$\frac{d}{dt} m_t = \lim_{N \rightarrow \infty} \sum_s p_t(s; m_t) \sum_i w_i(s) [F_i(s) - m_t] \quad (4)$$

$$p_t(s; m_t) = \frac{p_t(s) [F_t(s)]}{\sum_{s^0} p_t(s^0) [F_t(s^0)]} \quad (5)$$

Equation (4) still involves the conditional microscopic distribution $p_t(s; m_t)$. To proceed we follow [21, 22]: we (i) assume that the observables are self-averaging at all times (which one expects to be true), and (ii) approximate the microscopic measure $p_t(s; m_t)$ by the maximum entropy distribution given the condition that the microscopic observables take the value m_t . These assumptions imply that our observables evolve according to

$$\frac{d}{dt} m_t = m_t + \sum_z \frac{dh}{dz} D(h; m_t; e_t) \tanh(h) \quad (6)$$

$$\frac{d}{dt} e_t = 2e_t - \sum_z \frac{dh}{dz} D(h; m_t; e_t) h \tanh(h) \quad (7)$$

Here $D(h; m_t; e_t)$ denotes the asymptotic distribution of local fields in a system with magnetization m_t and energy e_t ,

$$D(h; m_t; e_t) = \lim_{N \rightarrow \infty} \frac{1}{N} \sum_{i=1}^N \frac{h}{\sum_{j=1}^N h_j} \ln \left[\frac{h}{h_k(s)} \right]_{m_t; e_t, \text{dis}} \quad (8)$$

where the average $[\cdot]_{m_t; e_t}$ is over the maximum entropy distribution given the values of the observables, viz. over

$$p(s; m_t; e_t) = \frac{p_t(s) [F_t(s)] [e_t - e(s)]}{\sum_{s^0} p_t(s^0) [F_t(s^0)] [e_t - e(s^0)]} \quad (9)$$

and $[\cdot]_{\text{dis}}$ is over the disorder (the realization of the random graph and bonds).

The relatively simple solution given in [23] can be understood within the current framework. Since all sites were identical, there was just a single cavity field and hence the distribution of local fields was uniform across sites and could be given explicitly in terms of the observables.

The field distribution $D(h; m_t; e_t)$ is readily calculated, even in the presence of bond or degree disorder, either via the replica method or via the cavity approach for dilute systems [15] (in the microcanonical or the canonical framework, respectively) [30]. Here the resulting equations from either approach are the same. They correspond to the maximum entropy distribution, given $(m_t; e_t)$, which equals the equilibrium distribution of a system with Hamiltonian (3) but with a pseudo inverse temperature $\hat{\beta}$ and pseudo external field $\hat{h} = \hat{h}$. The latter act as Lagrange parameters, enforcing the condition that the equilibrium distribution gives the required values of

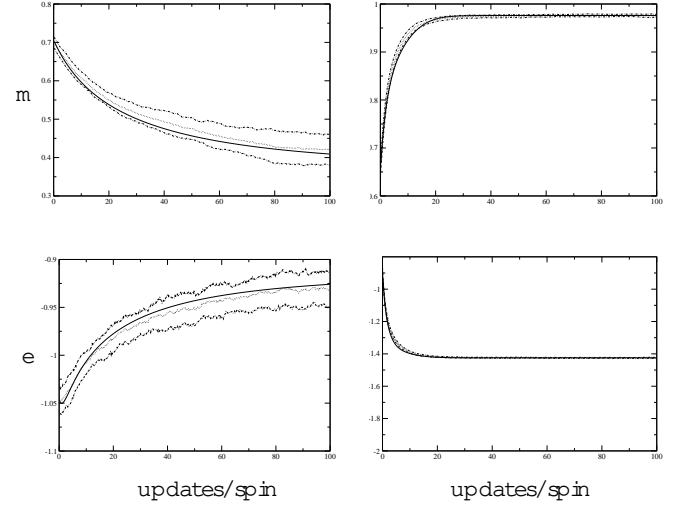


FIG. 1: Evolution of the magnetization m (top figures) and the energy e (bottom figures), for Ising spins on a 3-regular random graph with random bonds, and with time measured in units of updates per spin. Bond distribution: $Q(J) = (J-1) + (1-J)(J+1)$. Solid lines denote the theoretical predictions. Dotted lines represent the simulation data (system size $N = 10,000$ and averaged over 50 runs), with dot-dashed lines giving the averages ± 1 standard deviation. Left pictures: $\beta = 0.95$ and $\beta = 0.65$. Right pictures: $\beta = 0.97$ and $\beta = 1.2$.

$(m_t; e_t)$. The prefix ‘pseudo’ indicates that these parameters need not be physical: there could be states $(m_t; e_t)$ for which $\hat{\beta}$ is negative. Within the cavity formalism we can work either with the ensemble or with a particular realization of the disorder. The latter tends to be numerically simpler, due to the inherent (finite size) noise in population dynamics in the ensemble, which limits the accuracy with which the Lagrange parameters can be calculated. Working in areas of phase space where replica symmetry is expected to be exact and where belief propagation converges on any given graph realization, it is possible to find the Lagrange parameters to high precision. For large graph sizes the differences between results for graph realization and the ensemble average ought to vanish.

The resulting numerical algorithm is as follows. At any given point in time we know the instantaneous values $(m_t; e_t)$ of our observables. We then run a belief propagation algorithm on our graph, for a given pair of Lagrange parameters $(\hat{\beta}; \hat{h})$ which act as inverse temperature and external field; once the belief propagation has converged we can measure $(m_t(\hat{\beta}; \hat{h}); e_t(\hat{\beta}; \hat{h}))$. We now vary the Lagrange parameters and repeat the above until we satisfy the condition

$$m_t = m_t(\hat{\beta}; \hat{h}); e_t = e_t(\hat{\beta}; \hat{h}) \quad (10)$$

Finally we use the cavity fields generated with the correct values of $(\hat{\beta}; \hat{h})$ to give the local field distribution within our graph, with which we can evaluate the force terms in (6,7).

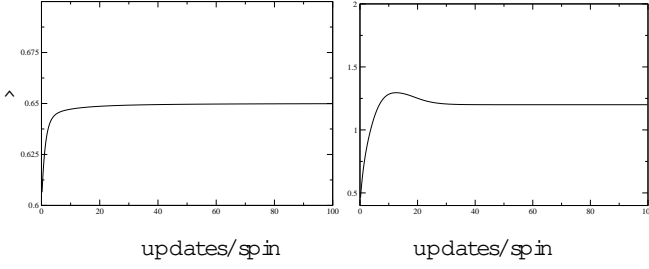


FIG. 2: Evolution of the inverse pseudo-temperature Lagrange parameter $\hat{\lambda}$ for the experiments shown in figure 1. Clearly, the relaxation of $\hat{\lambda}$ need not be monotonic.

In figure 1 we compare the results of our analysis with Monte Carlo simulations for a J spin-glass on a 3-regular graph. We sampled our graph uniformly from all connected graphs where each site has exactly three neighbours and each bond is drawn i.i.d. from $Q(J) = (J-1) + (1-J)(J+1)$. All simulations were carried out with a system size of $N = 10,000$, and were run on the same realization of the graph as the cavity field calculations. We see an excellent correspondence between theory and simulations. We have taken β to be relatively large (predominance of ferromagnetic bonds), since we did not wish to move into a region where belief propagation would not converge, a condition one expects to be closely related to instability in the AT sense [24, 25]. In such regions it is no longer possible to use belief propagation for accurately evaluating the Lagrange parameters $\hat{\lambda}$ and $\hat{\lambda}$.

It is also of interest to note in figure 2 that the evolution of the pseudo-temperature need not be monotonic. Assuming that the location of the AT line [24] is similar to that of the fully connected case, i.e. that it goes continuously from the zero-temperature instability ($T = 0$; $\beta = \frac{11}{12}$) [26, 27] to the triple point ($T = 1.13$; $\beta = 0.85$), as shown in [25], one could envisage a situation where starting from a replica symmetric (RS) phase, the parameters $(\beta; \lambda)$ could be chosen such that the final equilibrium phase was also RS, but where the dynamics would take the system through a regime of phase space where in equilibrium one would find replica symmetry breaking. Since there, the belief propagation (or any other replica symmetric) algorithm would not converge in a time of $O(N)$, the algorithm would become stuck en route to RS equilibrium.

In figure 3 we examine the order parameter ϕ in ferromagnetic random graphs with average connectivity 2 and 3, respectively. Here each bond is independently decided to be present ($c_{ij} = 1$) or absent ($c_{ij} = 0$) with probability c/N , where c is the average connectivity, leading to a graph with a Poisson degree distribution (or Erdos-Renyi graph). In these systems the inhomogeneity of the local environment of the spins is no longer caused by bond disorder, but by non-uniform connectivity. The agreement between theory and simulations in the case $c = 2$ is significantly worse than that in the other ex-

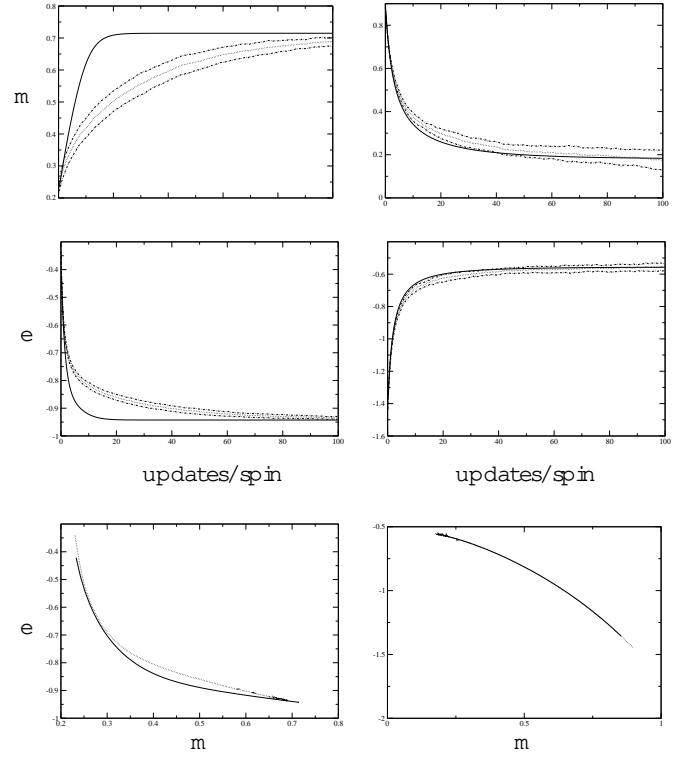


FIG. 3: Evolution of the magnetization m (top) and the energy e (bottom), for Ising spins on a Poisson random graph (of average connectivity c) with ferromagnetic bonds $J_{ij} = 1$, and with time measured in units of updates per spin (top 4 graphs) or ϕ in m space (bottom 2 graphs). Solid lines denote the theoretical predictions. Dotted lines represent the simulation data (system size $N = 10,000$ and averaged over 50 runs), with dot-dashed lines giving the averages ± 1 standard deviation. Left pictures: $c = 2$ and $T = 0.75$. Right pictures: $c = 3$ and $T = 2.8$.

amples presented. Here the maximum entropy measure appears to be a much less accurate approximation of the true microscopic distribution, which tells us that the system evolves through statistically atypical microscopic states, and predicts a relaxation of the order parameters that is far too quick. This would appear to be related to the increased heterogeneity associated with lower temperatures and lower average connectivity. However, plotting in the m plane we see that the predicted direction of the flow is still quite reasonable.

As a final example we turn to the decoding dynamics of finite connectivity Surlas codes [4, 5, 28] with 2-body interactions, which can easily be studied within the current framework. In particular, in figure 4 we consider the case of an unbiased source broadcasting through a binary symmetric channel with flip probability 0.04 and rate $\frac{2}{3}$ (the channel capacity as given by Shannon's theorem is 0.76...). If a message $(x_1; \dots; x_N)$ is sent across this channel, and our estimator for this message (given the corrupt channel) is given by $(\hat{x}_1; \dots; \hat{x}_N)$, then a natural performance measure is the overlap between the message sent and the decoded message, $O = N^{-1} \sum_i \hat{x}_i x_i$. We

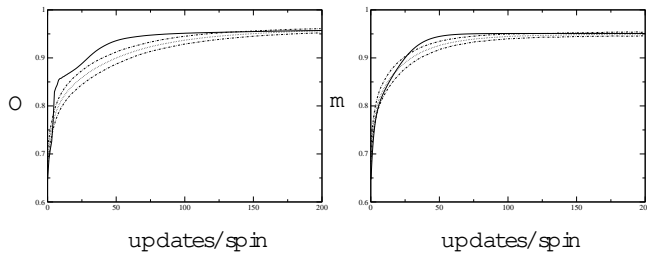


FIG. 4: Decoding dynamics of the overlap O (left) and the magnetization m (right), for a 2-body interaction and rate $\frac{2}{3}$ Sourlas error correcting code. Solid lines denote the theoretical predictions. Dotted lines represent the simulation data (system size $N = 10,000$ and averaged over 50 runs), with dot-dashed lines giving the averages ± 1 standard deviation. The temperature is Nishimori's temperature for the p probability (error rate) 0.04.

decode at Nishimori's temperature, which is the temperature maximizing this particular overlap observable [29] (the so-called maximizer of posterior marginals). Although qualitatively correct, the predicted relaxation of the order parameters is again too fast compared with the simulation data.

In this letter we have presented a relatively simple dynamical formalism, combining dynamical replica theory with the cavity method, to be used as a systematic approximation tool with which to understand the main features of the dynamics of dilute and disordered spin systems. We regard the wide applicability of the method as its strength. From the various applications presented here we see that our approach performs excellently in some cases, but relaxes too quickly in others, compared with numerical simulations. This is not unexpected [21]. However, as with the original dynamical replica theory, there is scope for increasing the order parameter set [22, 23], which should improve its accuracy systematically, albeit at a numerical cost. At present our method requires the convergence of belief propagation. It would therefore seem that breaking replica symmetry within this formalism will be non-trivial to implement, even though theoretically it is a straightforward generalization. For a single experiment we here run belief propagation $O(10^5)$ times; running a finite temperature 1RSB scheme that many times would be computationally extremely demanding without further approximations.

We warmly thank M. Okada, B. Wemmenhove and T. N. Ikoletopoulos for helpful discussions and comments.

^x Electronic address: hatchett@brain.riken.jp

^y Electronic address: isaac@thphys.ox.ac.uk

^z Electronic address: coolen@math.kcl.ac.uk

^x Electronic address: nikos@itf.fys.kuleuven.ac.be

- [1] M. Mezard, G. Parisi, and R. Zecchina, *Science* 297, 812 (2002).
- [2] R. Monasson, R. Zecchina, S. Kirkpatrick, B. Selman, and L. Troyansky, *Nature* 400, 133 (1999).
- [3] O. C. Martin, R. Monasson, and R. Zecchina, *Theoretical Computer Science* 265, 3 (2001).
- [4] Y. Kabashima and D. Saad, *Europhys. Lett.* 45, 97 (1999).
- [5] I. Kanter and D. Saad, *Phys. Rev. E* 61, 2137 (2000).
- [6] Y. Kabashima and D. Saad, *J. Phys. A: Math. Gen.* 37, R1 (2004).
- [7] M. Leone, A. Vazquez, A. Vespignani, and R. Zecchina, *Eur. Phys. J. B* 28, 191 (2002).
- [8] A. V. Goltsev, S. N. Dorojovtsev, and J. F. Mendes, *Phys. Rev. E* 67 (2002).
- [9] C. V. Giuraniuc, J. P. L. Hatchett, J. O. Indekeu, M. Leone, I. Perez Castillo, B. Van Schaeybroeck, and C. Vanderzande, *cond-mat/0408399* (2004).
- [10] B. Wemmenhove and A. C. C. Coolen, *J. Phys. A: Math. Gen.* 36, 9617 (2003).
- [11] I. Perez Castillo, B. Wemmenhove, J. P. L. Hatchett, A. C. C. Coolen, N. S. Skantzos, and T. N. Ikoletopoulos, *J. Phys. A: Math. Gen.* 37, 8789 (2004).
- [12] S. Galam, Y. Gefen, and Y. Shapir, *Math. J. Soc.* 9, 1 (1982).
- [13] L. Corrao, M. Leone, A. Pagnani, M. Weigt, and R. Zecchina, *cond-mat/0412443* (2004).
- [14] S. N. Dorojovtsev and J. F. F. Mendes, *Evolution of Networks* (Oxford University Press, Oxford, 2001).
- [15] M. Mezard and G. Parisi, *Eur. Phys. J. B* 20, 217 (2001).
- [16] M. Mezard and G. Parisi, *J. Stat. Phys.* 111, 1 (2003).
- [17] C. De Dominicis, *Phys. Rev. B* 18, 4913 (1978).
- [18] G. Semerjian and L. Cugliandolo, *Europhys. Lett.* 61, 247 (2003).
- [19] J. P. L. Hatchett, B. Wemmenhove, I. Perez Castillo, T. N. Ikoletopoulos, N. S. Skantzos, and A. C. C. Coolen, *J. Phys. A: Math. Gen.* 37, 6201 (2004).
- [20] J. P. L. Hatchett, in *Proceedings of CNET 2004* (2005).
- [21] A. C. C. Coolen and D. Sherrington, *J. Phys. A: Math. Gen.* 27, 7687 (1994).
- [22] S. N. Laughton, A. C. C. Coolen, and D. Sherrington, *J. Phys. A: Math. Gen.* 29, 763 (1996).
- [23] G. Semerjian and M. Weigt, *J. Phys. A: Math. Gen.* 37, 5525 (2004).
- [24] J. R. L. de Almeida and D. J. Thouless, *J. Phys. A: Math. Gen.* 11, 983 (1978).
- [25] Y. Kabashima, *Jour. Phys. Soc. Jpn.* 72, 1645 (2003).
- [26] C. Kwon and D. J. Thouless, *Phys. Rev. B* 37, 7649 (1988).
- [27] T. Castellani and F. Ricci-Tersenghi, *cond-mat/0403053* (2004).
- [28] T. Ozeki and M. Okada, *Prog. Theor. Phys. Suppl.* (to appear).
- [29] P. Rujan, *Phys. Rev. Lett.* 70, 2968 (1993).
- [30] Although the replica approach is more general since it does not require the existence of a Hamiltonian, i.e. it allows also for the study of systems without detailed balance.